[AMERICAN JOURNAL OF SCIENCE, SCHAIRER VOL. 267-A, 1969, P. 50-69]

ELECTRON-PROBE STUDY OF DIOPSIDE INCLUSIONS FROM KIMBERLITE

F. R. BOYD

Geophysical Laboratory
Carnegie Institution of Washington
Washington, D.C. 2008

ABSTRACT. Electron-probe analyses for ten elements have been made of six diopside inclusions from kimberlite, and forty-one additional specimens have been partially analyzed. Most of the diopsides are single crystals recovered from heavy mineral concentrates, but some are in nodules, and one formed an inclusion in diamond. Analyses for each element were made with reference to a single, usually synthetic standard, and corrections for drift, deadtime, background, absorption, fluorescence, and atomic number effects were made by computer. Analyses of known standards against known standards show that the accuracy obtained is normally better than ± 2 percent of the amount of an element present.

These diopsides show a wide range of solid solution toward enstatite, but the distribution of their Ca/(Ca + Mg) ratios is unexpectedly and asymmetrically bimodal. Forty-five of the diopsides have Ca/(Ca + Mg) ratios that cluster around 0.47, and the remaining two have ratios of 0.35. Quantitative comparisons with the diopside solvus in the synthetic system $MgSiO_3$–$CaMgSi_2O_6$ are subject to considerable uncertainty, but they suggest that the bulk of the kimberlite diopsides have equilibrated at temperatures of the order of 950° to 1000°C, whereas the two subcalcic specimens have equilibrated at temperatures in excess of 1300°C. Analyses for Fe show a pronounced maximum at 2.5 wt percent. There is a wide range in Al_2O_3 and Cr_2O_3 analyses, with broad maxima at 0.9 wt percent Cr_2O_3 and 1.6 wt percent Al_2O_3. It is suggested that these diopsides may have approached equilibrium more closely with enstatite than with garnet or spinel.

The diopside inclusion from a diamond crystal differs from the other samples in having very low Al_2O_3 and Cr_2O_3 and relatively high Fe and Mn.

INTRODUCTION

The mineral assemblages of peridotite nodules in kimberlite are notably simple. The most abundant primary minerals are forsterite, enstatite, and pyropic garnet, whereas diopside, phlogopite, and chrome spinel are less abundant. Mineralogic simplicity is combined with a coarse-grained fabric and a relative paucity of zoning and exsolution textures. It is very probable that these mineral assemblages represent subsolidus equilibria established at depth in the mantle and that the nodules have been only slightly affected by secondary processes during eruption. The simplicity of the assemblages offers the hope that they can be interpreted in detail with reference to experimental studies. Such interpretation would certainly contribute to an increased understanding of the origin of kimberlite itself and to our petrologic knowledge of the mantle as well.

Subsolidus phase studies of systems applicable to these peridotites have revealed one reaction and three solid solution relationships that are of particular interest. The reaction is enstatite + spinel $\rightleftarrows$ pyrope + forsterite, and it has been determined in the pure system MgO–Al_2O_3–SiO_2 by MacGregor (1964). This reaction, which separates the spinel peridotites from the garnet peridotites, is univariant for a range of bulk compositions in the more complex system CaO–MgO–Al_2O_3–SiO_2 (MacGregor, 1965), but in natural systems it may be considerably compli-

cated by the presence of chromium. The solid solution relationships of particular significance are the solid solution of enstatite in diopside (Davis and Boyd, 1966; Kushiro, 1968) and solid solutions of both enstatite and diopside toward garnet (Boyd and England, 1964; O'Hara and Yoder, 1967; Kushiro, Syono, and Akimoto, 1967). Variations in temperature and pressure markedly affect the compositional ranges of these solid solutions. Thus analytical data on the natural minerals combined with synthetic phase studies could, in principle, be used to fix the pressure-temperature conditions of equilibration of peridotite assemblages.

Clearly these phase studies are only a start, and their extension into more complex systems is needed. Nevertheless, progress in the interpretation of kimberlite peridotites is equally hampered by paucity of data on the chemical compositions of their constituent minerals. Figure 1 shows a compilation of modern wet-chemical analyses of diopsides from kimberlites. These analyses show a position and a trend that are very different from those found for Ca-rich pyroxenes that have crystallized from basaltic magmas. The kimberlite diopsides show no fractionation toward more Fe-rich compositions; instead they show a wide solid solution toward enstatite. The familiar trend of basaltic pyroxenes toward more Fe-rich compositions is due to equilibration with a liquid

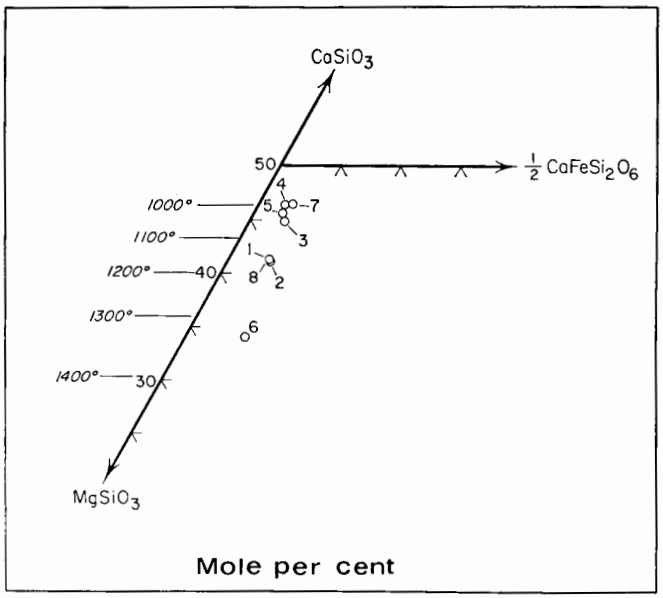

Fig. 1. Wet-chemical analyses of diopsides from kimberlites plotted in a portion of the pyroxene quadrilateral. Temperatures given are points on the diopside solvus in the system $MgSiO_3$–$CaMgSi_2O_6$ at 30 kb (Davis and Boyd, 1966). (1) ANU 2611, (2) ANU 2623, D. H. Green, personal commun.; (3) A.17, (4) A.3, O'Hara and Mercy (1963); (5) no. 7, Holmes (1936); (6) E.3, (7) G.12, Nixon, von Knorring, and Rooke (1963); (8) MacGregor and Ringwood (1964).

phase that varies in composition as cooling and fractionation proceed, whereas the trend of these kimberlite diopsides is evidently due to variable depth of subsolidus equilibration.

The study of diopside inclusions from kimberlite described in this paper was undertaken to extend the data provided by the wet-chemical analyses. Unfortunately, the material available for study at the initiation of the project was not ideal. Data are presented for diopsides from nine peridotite nodules. The remaining thirty-eight samples are predominantly single crystals picked from heavy-mineral concentrates formed in the process of recovery of diamonds from kimberlite, and so the particular mineral assemblages from which these crystals have come is not known. It is very likely, however, that they have crystallized in equilibrium with enstatite because whereas documented kimberlite nodules sometimes contain enstatite without diopside, only seldom do they contain diopside without enstatite. Brief descriptions of the nodules studied and of two single crystals of unusual composition are given in Appendix 1. Eight of the nodules are garnet lherzolites, and the ninth is a spinel lherzolite. Some of the garnet lherzolites also contain spinel, but in some cases it is difficult to be sure whether or not the spinel is primary.

Preliminary analytical data for most of these diopsides have been summarized in Annual Reports of the Director of the Geophysical Laboratory (Boyd, 1967, 1968). Results reported here supersede and differ slightly from those given in the Annual Reports because of the use of improved matrix corrections and because refinements in analytical technique have led to redetermination of samples studied in the early phases of the investigation.

A description of the analytical method used in this study, including tests made to determine its accuracy, is contained in Appendix 2. Most of the analyses are believed to be accurate to within ±2 relative percent.[1] Analyses for elements present in very minor or trace amounts are less accurate because of difficulties in determining background. In particular, the analyses for Mn in these diopsides are uncertain to ±5 to 10 relative percent, because of a problem in establishing the composition of the Mn standard.

Values of the ratio $\sigma / \sqrt{\bar{N}}$, where σ is the observed standard deviation and $\sqrt{\bar{N}}$ is the standard deviation predicted from counting statistics, are given along with the weight percentages of the major oxides in the complete analyses. A value for this ratio larger than 3 indicates that a particular element has an inhomogeneous distribution. Knowledge of inhomogeneity is valuable petrologic information, and it is an advantage of electron-probe analysis to be able to ascertain this property. However, this index, which can be termed a "homogeneity index", loses its sensitivity at low line/background ratios and hence cannot be used for trace elements.

[1] The term "relative percent" is used in this paper to mean percentage of the amount of an element or oxide present.

The electron-probe analyses reported here are based for the most part on synthetic standards prepared by J. F. Schairer. The precise techniques he has developed for preparation of silicate compositions have been needed to provide a sound basis for phase-equilibria studies. But it is hoped that he finds satisfaction in knowing that these same compositions are of immeasurable value as dependable standards for his colleagues in electron-probe laboratories.

ANALYTICAL RESULTS

Results of the partial and complete analyses of diopside inclusions from kimberlite are given in tables 1 and 2. The Ca/(Ca + Mg) ratios are of particular interest and are plotted in a histogram in figure 2.

TABLE 1

Partial analyses of diopsides from South African kimberlites

	Mine	Weight percent					Atomic percent			Atomic percent Ca/(Ca + Mg)
		Ca	Mg	Fe	Al	Cr	Ca	Mg	Fe	
75966-1	Bultfontein	16.0	10.2	3.1	0.1	0.4	46	48	6	49
75966-2	Bultfontein	14.3	9.9	1.4	1.3	1.6	45	51	3	47
75966-4	Bultfontein	14.2	10.2	2.5	1.0	0.8	43	51	5	46
75967-1	Bultfontein	14.9	10.3	2.5	0.9	0.6	44	50	5	47
75967-3	Bultfontein	14.6	9.9	2.6	1.0	0.7	45	50	6	47
75968-1	Bultfontein	13.8	9.8	2.5	1.1	0.9	44	51	6	46
75968-2	Bultfontein	14.4	10.0	2.4	0.9	0.7	44	51	5	47
75972-4	Wesselton	15.5	10.3	2.5	0.5	0.4	45	49	5	48
75973-1	Wesselton	14.2	10.0	2.5	1.0	0.7	44	51	6	46
75973-2	Wesselton	14.8	10.0	2.5	1.0	0.7	45	50	5	47
75974-1	Wesselton	13.8	9.8	2.7	1.2	0.8	43	51	6	46
75957-1	Kimberley	14.3	10.0	2.6	1.0	0.7	44	50	6	47
75957-2	Kimberley	13.8	9.8	2.7	1.2	0.9	43	51	6	46
75957-3	Kimberley	14.2	10.2	1.9	0.9	1.4	44	52	4	46
75957-4	Kimberley	15.4	10.3	2.4	0.7	0.5	45	50	5	48
75958-1	Kimberley	14.7	10.2	2.6	0.8	0.6	44	50	6	47
75958-2	Kimberley	14.2	9.9	2.8	1.0	0.7	44	50	6	47
75958-3	Kimberley	14.7	10.1	2.4	1.0	0.7	44	50	5	47
75959-1	Kimberley	14.5	10.2	2.4	0.9	0.8	44	51	5	46
75959-2	Kimberley	15.3	10.4	2.4	0.8	0.5	45	50	5	47
75959-3	Kimberley	15.1	10.2	2.4	0.9	0.7	45	50	5	47
75938-1	De Beers	15.5	10.3	2.4	0.7	0.5	45	50	5	48
75938-2	De Beers	14.4	10.2	2.0	0.7	1.5	44	52	4	46
75938-3	De Beers	14.9	10.2	2.3	0.8	0.9	45	51	5	47
75938-4	De Beers	14.8	10.1	1.6	0.6	1.9	46	51	4	47
75936-1	De Beers	14.4	10.0	2.2	0.9	1.3	44	51	5	47
75936-2	De Beers	15.1	10.3	2.5	1.1	0.6	45	50	5	47
75936-3	De Beers	15.3	10.3	2.5	0.7	0.6	45	50	5	48
73191-1	De Beers	12.7	9.6	2.5	1.7	1.1	42	52	6	45
73191-2	De Beers	15.9	10.6	2.4	0.4	0.4	45	50	5	48
73191-3	De Beers	15.3	10.4	2.4	0.7	0.4	45	50	5	47
73191-4	De Beers	14.9	10.3	2.5	0.8	0.6	44	51	5	47
75937-1	De Beers	15.3	10.7	2.2	0.7	0.6	44	51	5	47
75937-2	De Beers	15.0	10.4	2.4	0.8	0.6	45	51	5	47
75937-3	De Beers	14.3	10.3	2.6	0.9	0.6	43	51	6	46
87703	De Beers	15.1	10.2	2.5	0.7	0.5	44	51	5	46
DB-2	De Beers	14.7	11.0	...	...	...	...	...	...	45
L-3	Lauwrencia	15.0	10.5	...	...	...	...	...	...	47
K-29	Kamfersdam	13.2	9.3	...	...	...	...	...	...	46
W-46	Wesselton	13.8	9.2	...	...	...	...	...	...	48
D-26	Dutoitspan	13.9	10.2	...	...	...	...	...	...	45

Analyses 75966-1 through 87703 are for single crystals from the collection of the U. S. National Museum. DB-2 through D-26 are from nodules described in Appendix 1.

TABLE 2

Electron-probe analyses of diopsides from South African kimberlites

	E-3		PHN-4		M-72		E-11		MM-4		M	
SiO_2	55.2	2	54.3	2	54.6	3	54.2	2	54.9	2	52.8	4
TiO_2	0.16	...	0.13	...	0.15	...	0.41	...	0.003	...	0.43	29
Al_2O_3	2.05	8	2.39	2	2.10	20	3.03	5	2.93	6	0.86	74
Cr_2O_3	0.85	2	0.79	2	3.15	50	1.45	4	1.82	27	0.09	...
FeO*	3.34	2	4.04	1	2.13	7	2.59	2	2.14	3	5.89	41
MnO	0.12	...	0.14	...	0.09	...	0.09	...	0.08	...	0.71	57
CaO	16.1	2	15.4	2	19.9	4	19.5	3	20.1	6	20.9	7
MgO	21.2	1	20.9	1	16.1	3	17.3	2	16.6	2	16.1	5
Na_2O	1.24	1	1.52	1	2.50	7	1.95	2	2.31	5	1.38	10
K_2O	0.05	...	0.04	...	0.01	...	0.01	...	<0.003	...	<0.004	...
Totals	100.4		99.7		100.7		100.6		101.0		99.2	

*Total Fe as FeO.

Values for the ratio $\sigma/\sqrt{N}$ are underlined.

See Appendix 1 for descriptions of these specimens.

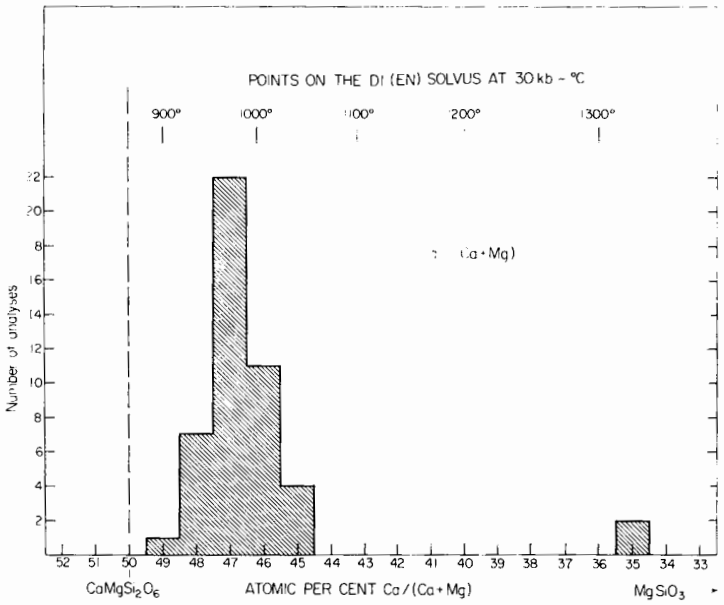

Fig. 2. Ca/(Ca + Mg) ratios of the diopsides from kimberlite listed in tables 1 and 2.

Inasmuch as these diopsides contain some Fe, the points plotted in figure 2 are actually projections from the $FeSiO_3$ corner of the pyroxene quadrilateral onto the join $CaMgSi_2O_6$–$MgSiO_3$. The amount of Fe in these diopsides is small (~5 mole percent $FeSiO_3$), however, and because of their close grouping it is impracticable to plot the analyses in the quadrilateral.

The histogram in figure 2 shows a curious bimodal distribution, very different from that anticipated from the distribution shown by the limited number of wet-chemical analyses in figure 1. Forty-five of the total of forty-seven analyses have Ca/(Ca + Mg) ratios that cluster around a value of 0.47, whereas the remaining two show a high degree of solid solution toward enstatite, with Ca/(Ca + Mg) ratios of 0.35. The uncertainty in this ratio is about 0.01. For example if the weight content of Ca in one of these analyses were decreased by 2 relative percent and the weight content of Mg were increased by 2 relative percent, the Ca/(Ca + Mg) ratio would be changed by 0.01.

Histograms in figures 3, 4, and 5 show the variations in the weight contents of Fe, Al_2O_3, and Cr_2O_3. The Fe analyses show a pronounced maximum at 2.5 wt percent Fe with substantial scatter to higher and lower values. Results for Al_2O_3 and Cr_2O_3 show broad maxima at 1.6 wt percent Al_2O_3 and 0.9 wt percent Cr_2O_3. The range in Al_2O_3 content is a factor of 10, and in Cr_2O_3 a factor of 30. If the inclusion from diamond (sample M), which is very poor in Cr_2O_3, is excluded from this group, the range in Cr_2O_3 content becomes a factor of 6. In these

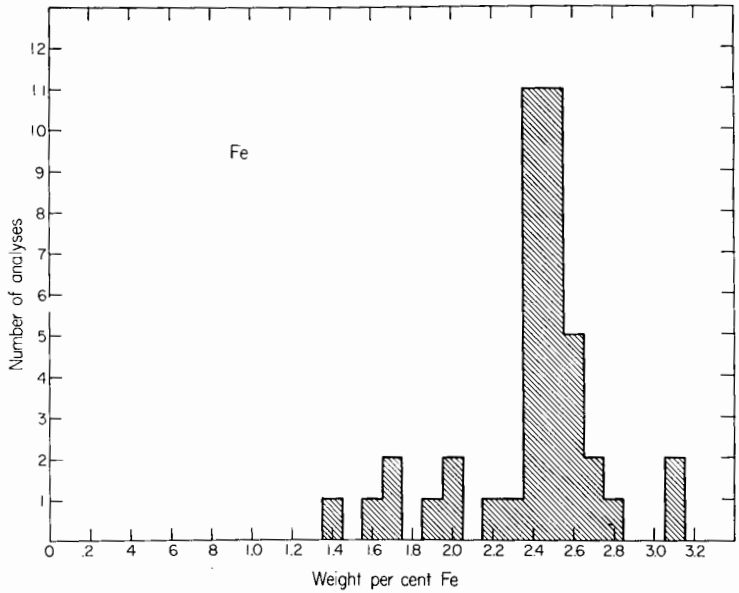

Fig. 3. Fe contents of diopsides from kimberlite. Numerical measurements are given in tables 1 and 2.

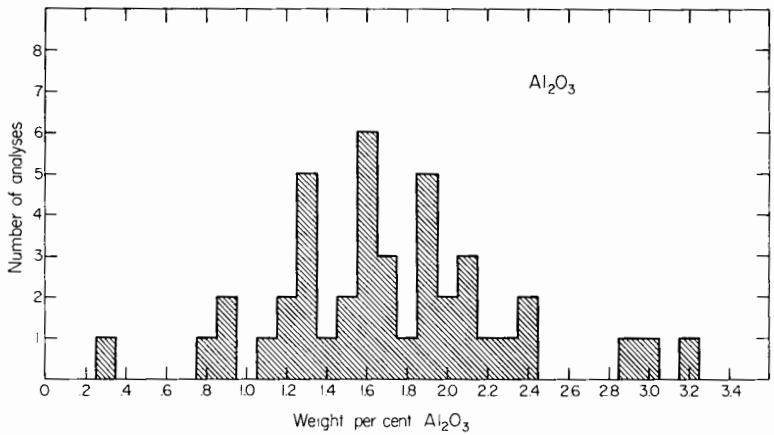

Fig. 4. Al_2O_3 contents of diopsides from kimberlite. Numerical data are given in tables 1 and 2.

histograms for Fe, Al_2O_3, and Cr_2O_3 there is no suggestion of the bimodal distribution shown by the Ca/(Ca + Mg) ratios.

The six complete analyses in table 2 all total between 99.0 and 101.0, indicating that the matrix corrections used work well. Values for the ratio $\sigma/\sqrt{N}$ (homogeneity index) show that, with the exception of the inclusion from diamond, these diopsides are relatively homogeneous. This is particularly true of the two subcalcic diopsides, one of which

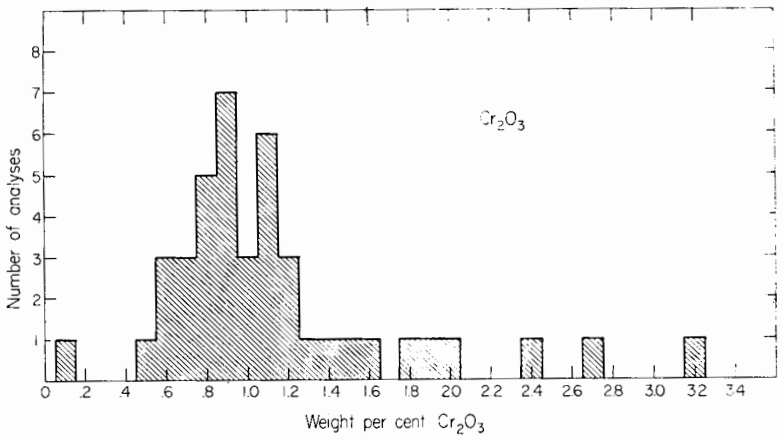

Fig. 5. Cr_2O_3 contents of diopsides from kimberlite. Numerical data are given in tables 1 and 2.

(PHN-4, Shinyanga) is completely homogeneous insofar as can be discerned by the probe with a 10-μm beam. This relative homogeneity is consistent with a high equilibration temperature, suggested by the large solid solution toward enstatite exhibited by these two pyroxenes. It also implies a rapid cooling during eruption of the kimberlite. In most of the six analyses, inhomogeneities in Al and Cr distribution are more pronounced than for other elements. The trivalent ions are more strongly bonded in the pyroxene structure than divalent ions such as Ca, Mg, and Fe, and it is probable that these inhomogeneities are primary. No regular zoning in the distribution of Al and Cr was noted, however.

The potassium content of these pyroxenes is of interest inasmuch as it is difficult to understand how the large K ion can fit in the diopside structure. X-ray studies by J. Papike (personal commun.) have shown that some omphacites and other pyroxenes apparently rich in K_2O are actually intergrown with secondary (?) amphibole. Four of the analyzed diopsides show significant K contents in the range 90 to 390 ppm, whereas in the other two potassium was not detected. The detectable limit for K under the conditions of these analyses was estimated from Student's t and found to be about 20 ppm.

The two subcalcic diopsides contain the most potassium (330 and 390 ppm), and this may be a reflection of their unusually high equilibration temperature. The Shinyanga diopside (PHN-4) showed a few small optical inhomogeneities, and probe profiles for K were run across them to see if possibly the potassium might be localized in secondary amphibole. However, no anomalies in the potassium distribution were found.

The complete analyses are recalculated as pyroxene formulae on the basis of six oxygens in table 3. The lack of Al substituting for Si is striking, inasmuch as all of these diopsides contain 1.95 or more atoms of Si per formula unit. This relationship is consistent with their

TABLE 3

Diopside structure formulas calculated on the basis of six oxygens

	E-3		PHN-4		M-72		E-11		MM-4		M	
Si	1.97		1.96		1.97		1.95		1.97		1.97	
Ti	0.004	2.000	0.004	2.000	0.004	2.000	0.011	2.000	...	2.000	0.012	2.000
Al	0.026		0.036		0.026		0.039		0.030		0.018	
Al	0.060		0.066		0.063		0.089		0.094		0.020	
Cr	0.024		0.023		0.090		0.041		0.051		0.003	
Fe*	0.100		0.122		0.064		0.078		0.064		0.183	
Mn	0.004	2.022	0.004	2.038	0.003	2.030	0.003	2.027	0.002	2.032	0.022	2.057
Mg	1.13		1.12		0.865		0.927		0.888		0.895	
Ca	0.616		0.595		0.769		0.752		0.773		0.834	
Na	0.086		0.106		0.175		0.136		0.160		0.100	
K	0.002		0.002		0.001		0.001		...		...	
Ca	0.335		0.324		0.453		0.428		0.448		0.436	
Mg	0.611		0.610		0.510		0.527		0.515		0.468	
Fe	0.054		0.066		0.038		0.044		0.037		0.096	
Ca/(Ca + Mg)	0.354		0.347		0.470		0.448		0.465		0.482	

*Total Fe as Fe^{++}.

See Appendix 1 for descriptions of these specimens.

supposed formation at considerable depth in the mantle. High pressure in excess of that required to stabilize garnet tends to reduce the solubility of Al in four-fold coordination in pyroxene and to increase the amount of garnet in which the Al is entirely in six-fold coordination (Boyd and England, 1964; Kushiro, Syono, and Akimoto, 1967).

The Fe in these analyses has been recalculated as if it were entirely divalent. Obviously this is not true, and the slight excess in total atoms in the M1 and M2 sites, which is present in all the analyses, is due in part to this error. Lack of knowledge of ferric iron content prevents a detailed charge balance, but if a portion of the Al^{VI} is taken to balance Al^{IV}, the sum of the remaining Al^{VI} and Cr is less than the number of atoms of Na in all the analyses. This relationship indicates the presence of some ferric iron.

The E-3 subcalcic diopside has been analyzed by wet-chemical means (Nixon, von Knorring, and Rooke, 1963) as well as by the electron probe in the present study. The probe results and the wet-chemical analysis are compared in table 4. The agreement is within ±2 relative percent for the major oxides CaO, MgO, and SiO_2, but there are significant discrepancies in the analyses for Al_2O_3, FeO, and K_2O.

TABLE 4

Analyses of the E-3 subcalcic diopside

	Probe	Wet chemical*
SiO_2	55.2	54.61
TiO_2	0.16	0.23
Al_2O_3	2.05	1.30
Cr_2O_3	0.85	0.92
FeO†	3.34	4.04
MnO	0.12	0.10
MgO	21.2	20.88
CaO	16.1	16.20
Na_2O	1.24	1.28
K_2O	0.05	0.12
Totals	100.4	99.68

*Analyst: M. H. Kerr (Nixon, von Knorring, and Rooke, 1963). Original analysis gives FeO, 3.02; Fe_2O_3, 1.14; H_2O^+, 0.41; H_2O^-, 0.10; total, 100.28.

†Total Fe as FeO.

DISCUSSION

The distribution of Ca/(Ca + Mg) ratios of these diopsides makes it appear that all but two of the forty-seven specimens came from a restricted depth range in the mantle, but that these remaining two came from a considerably greater depth, where the temperature was about 300°C higher. This is a surprising result. It may well be that the bimodal distribution is an accident of sampling and that it will not prove to be true for diopsides from South African kimberlites in general. A more expected distribution would be a peak in the Ca/(Ca + Mg) ratios at a particular temperature, with a gradual trailing off toward higher temperatures. In other words, it might more reasonably be believed that most kimberlites were erupted from a restricted depth range in the mantle, with a progressively decreasing number coming from progressively increasing depth. That this may well be the case is suggested by three of the diopsides analyzed by wet-chemical methods (fig. 1), which have Ca/(Ca + Mg) ratios of 0.43, intermediate between the two groups of samples analyzed with the probe.

There is also a geographic bias in the data. Forty of the forty-five samples with Ca/(Ca + Mg) ratios clustering around 0.47 are from pipes in the Kimberly area. One of the subcalcic specimens is from the Shinyanga diamond field in Tanzania, and the other is from the Thaba Putsoa pipe in Lesotho (Basutoland). It would be interesting to have data for a number of diopsides from the same pipe as well as a broader geographic distribution of samples.

Equilibria between diopside and garnet or diopside and spinel control the solubility of Al_2O_3 and Cr_2O_3 in the diopside in the same manner that equilibrium between diopside and enstatite controls the Ca/(Ca + Mg) ratio. Both Al_2O_3 and Cr_2O_3 analyses show considerable scatter, with no suggestion of the bimodal distribution found for the Ca/(Ca + Mg) ratios). Unfortunately, the specific assemblages in which most of these diopsides formed is not known, and it may be that some of the variations in Al_2O_3 and Cr_2O_3 are due to variations in phase assemblage. But it can be noted in table 2 that Al and Cr are considerably more likely to have inhomogeneous distributions in a given sample than are the other elements. Hence it may be that the approach to equilibrium between diopside and spinel or garnet is less complete than between diopside and enstatite and this is least partly responsible for the range in Al_2O_3 and Cr_2O_3 values.

The diopside inclusion from a diamond crystal (sample M) differs in composition from the other analyzed specimens in a number of ways. It contains considerably more Fe and Mn and notably less Al and Cr than the others. The Cr content (650 ppm) is particularly low. This diopside shows little solid solution toward enstatite [Ca/(Ca + Mg) = 0.48], and it is very inhomogeneous. The inclusion is one of two diopside crystals from a single diamond host, and it was removed from the diamond at University College London by fracturing the diamond. Some surface alteration, believed to be kaolinite, was found on it (H. J.

Milledge, personal commun.). The kaolinite presumably formed by secondary alteration through cracks in the diamond, and some of the inhomogeneity might be due to this alteration.

Meyer (1968) has found that some garnet inclusions from diamond are much richer in Cr than the usual, pyrope-rich garnets from the kimberlite nodules. They contain up to 30 percent of the $Mg_3Cr_2Si_3O_{12}$ end member. These inclusions are always monomineralic, and it is problematical whether they can be regarded as derived from equilibrium mineral assemblages. If the Cr-rich garnet and the diopside poor in Al and Cr have formed in equilibrium, however, it is clear that this assemblage must have formed under different pressure-temperature conditions than the minerals of the nodules. In the system enstatite-pyrope (Boyd and England, 1964), increasing the pressure reduces the solubility of Al in the pyroxene and leads to the formation of more garnet. An analogous effect is possible for Cr in diopside and garnet.

The diopside solvus in the system $MgSiO_3$–$CaMgSi_2O_6$ is apparently little affected by pressure (Davis and Boyd, 1966). Points from the determination of this solvus at 30 kb are shown in figures 1 and 2 along with analytical data on the diopside inclusions from kimberlite. It is interesting to compare these data, but it must be understood that the uncertainties in such comparisons are at present quantitatively unknown. The presence of Al, Cr, Fe, and other ions in the natural pyroxenes can be expected to affect their solid solution relations. O'Hara and Yoder (1967) have obtained data which suggest that solution of Al in diopside and enstatite broadens the two-pyroxene field. As these phase studies are extended and refined it clearly will be possible to make more precise estimates of equilibriation temperatures than can presently be done.

The two subcalcic diopsides (E-3 and PHN-4) show a more extensive solid solution with enstatite than any other Fe-poor diopsides known to the author. They are coarse-grained, homogeneous minerals, and there can be little doubt that they formed as stable phases. They and most other diopsides from kimberlites differ markedly from Ca-rich pyroxenes from gabbroic rocks in that they show no exsolution lamellae. Hence, the eruption of the kimberlite from the mantle into the crust must have been rapid enough to quench them from an equilibration temperature which for these two diopsides appears to have been of the order of 1300°C (fig. 2). The enstatite that crystallized with the E-3 diopside has been analyzed (Nixon, von Knorring, and Rooke, 1963), and it is interesting to note that it has a higher Ca/(Ca + Mg) ratio (2.8 atomic percent Ca) than other enstatites from kimberlite thus far studied. This fact is further evidence of an unusually high equilibration temperature, although the enstatite solvus in the system $CaMgSi_2O_6$–$MgSiO_3$ is not so sensitive to temperature as the diopside solvus.

ACKNOWLEDGMENTS

It is a particular pleasure to acknowledge the persistent effort and skill of C. G. Hadidiacos in maintaining and improving the electron probe used in this investigation. L. W. Finger and F. Chayes provided

invaluable aid in developing the computer programs used in reducing the probe data. J. I. Goldstein, K. Frederiksson, and C. Taylor have generously given advice on electron-probe technology and have reviewed portions of this work as it appeared in the Annual Reports of the Director of the Geophysical Laboratory. I. MacGregor, P. H. Nixon, W. G. Melson, H. J. Milledge, and H. S. Yoder provided the specimens that were analyzed. J. F. Schairer, E. G. Zies, and C. O. Ingamells assisted in various ways in the search for better standards. The final manuscript has benefited greatly from critical reviews by G. M. Brown and H. S. Yoder.

APPENDIX 1

DESCRIPTION OF SAMPLES

Most of the samples analyzed in this investigation are single crystals of chrome diopside, 2 to 10 mm in diameter, picked from heavy-mineral concentrates. They require no detailed description. However, brief petrographic descriptions are given for nine peridotite nodules in which the diopsides were partially or completely analyzed. Descriptions are also given of two diopside crystals of unusual composition.

E-3.—Subcalcic diopside in lherzolite nodule from Thaba Putsoa pipe, Lesotho (Basutoland). The other primary minerals are forsterite, enstatite, and pyrope. A mode of this nodule together with wet-chemical analyses by M. H. Kerr of the diopside, enstatite, and pyrope, and a whole-rock analysis of the nodule are given in Nixon, von Knorring, and Rooke (1963). This nodule is relatively fine grained and little altered. The diopside is abundant.

PHN-4.—Subcalcic diopside, single crystal about 3 mm in diameter. Shinyanga diamond field, Tanzania. The crystal is from the collection of the Uganda Geological Survey. Optically there appears to be slight alteration along cleavages, but there are no exsolution lamellae and the probe counts show the crystal to be unusually homogeneous.

E-11.—Diopside from lherzolite nodule, Farm Lauwrencia, S. W. Africa. The other primary minerals are forsterite, enstatite, and pyrope. A mode of this nodule and wet-chemical analyses by M. H. Kerr of the whole nodule and the pyrope are given by Nixon, von Knorring, and Rooke (1963). The probe analysis was carried out on a partial separation of the diopside prepared as a grain mount.

M-72.—Chrome diopside in lherzolite nodule, Monastery Mine, Southeast Free State. The other primary minerals are forsterite, enstatite, spinel, phlogopite, and minor pyrope. The diopside is mostly intergrown with phlogopite and spinel in interstitial aggregates between larger grains of forsterite and enstatite.

MM-4.—Chrome diopside in lherzolite nodule, Malibo Matso pipe, Lesotho. The nodule is composed predominantly of olivine and enstatite with minor diopside, pyrope, and spinel.

DB-2.—Diopside in mylonitized lherzolite, De Beers pipe, Kimberly. Coarse forsterite and enstatite grains with undulate extinction are embedded in a granulated matrix of these same minerals. The pyrope is much altered, and there is some, apparently secondary, spinel. The diopside is very sparse.

D-26.—Chrome diopside in lherzolite nodule, Dutoitspan mine, Kimberley. This nodule contains coarse forsterite, enstatite, and diopside and small garnets with kelyphite rims. There are minor, probably secondary, phlogopite and spinel.

W-46.—Chrome diopside in spinel-lherzolite nodule, Wesselton mine, Kimberley. Sparse Cr-rich diopside is present with forsterite, enstatite, phlogopite, and minor spinel.

K-27.—Diopside in altered lherzolite nodule, Kamfersdam pipe, Kimberley. This nodule also contains olivine, enstatite, garnet, and sparse phlogopite and spinel.

L-3.—Diopside in much altered lherzolite nodule, Farm Lauwrencia, S. W. Africa. Olivine, enstatite, garnet, and minor phlogopite and spinel are also present.

M.—Diopside inclusion in diamond, locality unknown. This inclusion is one of two from a single diamond. It was borrowed from University College London, through

the courtesy of Dr. H. Judith Milledge. The inclusion is tabular parallel to 100 and about 300 μm long. It has been mounted in epoxy and was polished several times during analysis. There has been some surficial alteration to kaolinite.

APPENDIX 2

ANALYTICAL METHOD

Instrument

The analyses reported in this paper were made with a Materials Analysis Company Model-400 electron probe.[1] This instrument has a take-off angle of 35° and an angle of incidence of the beam to the specimen surface of 62½°. Data for quantitative analyses are simultaneously read out on an automatic typewriter and a card punch. These data include the output of three channels with scale factors, the counting interval, the specimen current, and a sequence of code numbers which identify the elements being analyzed, the standards used, and the type of measurement being made. The data translator supplied with the probe was modified extensively to provide this capacity.

Correction Procedure

Reduction of X-ray intensity measurements to chemical composition requires correction for differential generation, absorption, and fluorescence effects. Various empirical and theoretical solutions to the problem of correcting X-ray intensities have been proposed, and currently there is active debate over which are superior. At the present time there have been insufficient tests to make possible a clear choice between correction procedures. Nevertheless, an adequate justification for the use of particular matrix corrections can be solely that they provide sufficient accuracy in any given investigation. Analyses of known standards against other known standards, described below, indicate that with the correction procedures used an accuracy better than ± 2 relative percent has been achieved in most, but not all cases. This uncertainty approaches the limit that can be obtained with modern electron probes. In general, standards have been selected so that the matrix corrections are kept small, usually less than 10 relative percent. Nevertheless, absorption corrections up to 30 relative percent are present in some of the standard analyses discussed below, and the results are still correct within ± 4 relative percent.

The absorption correction of Philibert (1963) with the overvoltage modification of Duncumb and Shields (1963) has been used. However, constants in the equation for the Leonard coefficient (σ) have been taken from the recent work of K. J. F. Heinrich[2] (personal commun.). Choice of constants in calculating σ makes a significant difference. For example, the mean total of the first five analyses in table 10 is 100.5. If the constants of Duncumb and Shields are used, the mean total of these analyses becomes 100.9. Mass absorption coefficients are taken from Heinrich (1966).

The fluorescence correction of Reed (1965) has been used, and the simplifications that he suggested for calculating the term $(r_A - 1)/r_A$ and for the fluorescence yield, $W_K(B)$, are followed. Atomic number effects oppose each other, but their resultant can be significant. The recent treatment by Duncumb and Reed (1968) has been used. Duncumb has also made available an equation for calculating the backscatter factor, R. This equation is too complex to be used with a desk calculator, but it can be programmed for a large computer.

Both the Philibert expression for absorption and the Castaing-Reed expression for fluorescence contain the term cosec θ, where θ is the take-off angle. To allow for the inclined incidence of the beam to the specimen surface in the M.A.C. probe, the term cosec θ is replaced by sin θ_1 cosec θ_2, where θ_1 is the angle of incidence and θ_2 is the take-off angle.

The degree of automation in the reduction of intensity measurements was greatly increased during the period in which these data were being obtained. The most recent results have been read out from the probe with a card punch, and all reduction is now effected with programs written for a Univac 1108 in Fortran IV. It was found convenient to effect this reduction with two programs. With the first of these, CONE, raw counts are averaged, and corrections are made for background, deadtime, and drift. A homogeneity index is also computed for each group of counts, and in the

[1] The assistance of the National Science Foundation in the purchase of this instrument under grant GP 4384 is gratefully acknowledged.

[2] With Heinrich's coefficients $\sigma = 4.25 \times 10^5/(V_o^{1.65} - V_c^{1.65})$.

event that an element is present at a concentration less than 0.1 percent, Student's t is used to calculate a detection limit. A second program, ABFAN, is used to make the matrix corrections outlined above, iterating to refine the various correction factors. All the anlyses given in this paper have been corrected by using ABFAN. Boyd, Finger, and Chayes (1968) have described these programs more fully.

Standards

A variety of glasses prepared by J. F. Schairer have been used as standards for Na, Mg, Al, Si, and Ca. Experience has shown that they are homogeneous. The accuracy to which the compositions of these glasses are known is difficult to establish in an absolute way, but it is considerably better than the accuracy that can be obtained with an electron probe. Hence analyses between these standards provide an indication of the over-all accuracy of the probe analyses and a check on the correction procedures.

In the tables of data that follow, the factors listed under the heading "Matrix correction" include all absorption, fluorescence, and atomic number effects. Initial compositions obtained from intensity ratios are multiplied by these factors to give the corrected compositions. In cases where complete analyses have been made of unknown samples, the matrix correction factors have been formed by iteration, starting with initial approximations to the compositions. For many of the standard analyses, however, the expected compositions were used to calculate the matrix corrections. As will be shown, these two procedures give the same result.

TABLE 5

Analyses of pure $CaMgSi_2O_6$ glass, with

$CaSiO_3$ and $MgSiO_3$ glass as standards

	Standard	Matrix correction	Weight percent	
			Probe	Expected
CaO	$CaSiO_3$	1.019	26.4	25.90
MgO	$MgSiO_3$	1.074	18.4	18.62
SiO_2	$CaSiO_3$	1.066	55.8	55.48
	$MgSiO_3$	0.928	54.7	
Totals			100.1*	100.00

*Total includes mean of SiO_2 analyses.

Table 5 shows analyses of pure diopside glass, with $MgSiO_3$ glass and $CaSiO_3$ glass as standards. The matrix corrections are predominantly for absorption and range from 2 percent for Ca to 7 percent for Mg. The probe results agree with the expected compositions within ± 2 relative percent. Table 6 shows analyses of two glasses in the system MgO–Al_2O_3–SiO_2, with a third glass in this system as a standard. Here the matrix effects are less than 5 percent, and the agreement between the probe analyses and expected compositions is again within ± 2 relative percent.

Table 7 gives analyses of these same two glasses and their glass standard, this time with pure synthetic periclase and corundum, and pure natural quartz as standards. The matrix corrections are again predominantly for absorption and are rather large, particularly for Si and Al. The differences between the probe analyses and expected compositions are as large as 4 relative percent, but for many purposes this would be adequate. Clearly, matrix corrections should be kept small if the maximum possible accuracy is desired.

A test of the iteration procedure is also given in table 7. Column A under "Matrix correction" gives factors obtained from the expected compositions, and column

TABLE 6

Analyses of two glasses on the join $MgSiO_3$-Al_2O_3, with a third glass on this join, containing 5.00 percent Al_2O_3 as a standard

	Matrix correction	Weight percent	
		Probe	Expected
MgO	0.966	36.8	36.14
SiO_2	1.016	54.0	53.86
Al_2O_3	0.990	10.1	10.00
Totals		100.9	100.00
MgO	0.993	32.7	32.13
SiO_2	1.044	48.2	47.87
Al_2O_3	0.964	20.1	20.00
Totals		101.0	100.00

B shows factors obtained by iteration. It can be seen that the two procedures give virtually identical results and the simple iteration method evidently works. Program ABFAN prints out the number of iterations required to give a composition that differs from the composition on the previous cycle by less than 0.1 relative percent of any of the elements present. Usually three iterations are sufficient, and never have more than five been required.

Analyses for sodium are difficult because it volatilizes readily under the electron beam, particularly from glasses. Nevertheless, this difficulty can be reduced to a negligible level by keeping the specimen current below 0.1 μa and using a beam diameter of 15 to 20 μm. A smaller beam can be used on crystalline materials. Two analyses of glasses containing Na and of a natural jadeite analyzed by E. G. Zies are shown in table 8. Differences between expected and obtained results are within ± 2 relative percent for the glasses, but the jadeite analysis is in error by 3 relative percent. Counts on the jadeite were rather variable, possibly owing to an unusually irregular topography on the sample surface.

Synthetic standards containing the transition elements are very difficult to prepare because these elements tend to volatilize and dissolve in platinum containers. The problem was avoided for an iron standard by using a natural forsterite from Balsam Gap, North Carolina, which was analyzed by wet-chemical methods for total iron and FeO by E. G. Zies. The means of multiple analyses that agree within 0.08 percent gave 7.28 percent total iron as FeO and 6.90 percent FeO.

Oxygen is evolved in the reactions by which transition elements in solution in silicate liquids reduce and dissolve in platinum. These reactions are inhibited by preparing samples at high confining pressures, where systems approach a closed state. Glasses containing small amounts of Cr and Mn have been prepared in this way and were used as standards for these elements in the present study. Control on the composition of these glasses is inherently less accurate, however, than with the preparation techniques used at atmospheric pressure by J. F. Schairer, partly because very small samples must be used in the high-pressure apparatus and partly because changes in composition at high temperature are not completely eliminated by high pressure.

A glass containing Cr was prepared by dissolving Cr_2O_3 in a liquid with the composition 75 $CaMgSi_2O_6$, 25 $MgSiO_3$ (wt percent) at approximately 1800°C and

TABLE 7

Analyses of three glasses on the join $MgSiO_3$-Al_2O_3, with pure MgO, SiO_2, and Al_2O_3 as standards

	Matrix correction		Weight percent	
	A	B	Probe	Expected
MgO	1.064	1.063	37.1	38.15
SiO_2	1.197	1.201	58.0	56.85
Al_2O_3	1.296	1.289	5.1	5.00
Totals			100.2	100.00
MgO	1.059	1.062	35.9	36.14
SiO_2	1.217	1.218	54.9	53.86
Al_2O_3	1.283	1.287	10.4	10.00
Totals			101.2	100.00
MgO	1.056	1.059	31.8	32.13
SiO_2	1.252	1.252	49.1	47.87
Al_2O_3	1.249	1.254	20.5	20.00
Totals			101.4	100.00

A. By iteration from initial approximation to the composition.

B. From expected composition.

11 kb. The nominal composition of the glass included 1.31 percent Cr. To check this composition the glass was analyzed with the probe relative to a chromite (52 NL 11) provided by E. D. Jackson. The mean of six analyses that were consistent gave 1.28 percent Cr.

An Mn-bearing glass was prepared under similar conditions by dissolving $MnSiO_3$ in a liquid of pyrope ($Mg_3Al_2Si_3O_{12}$) composition. The nominal composition of this glass contained 4.19 percent Mn. Checks were made on its composition by using it to analyze natural minerals with a wide range of manganese contents, and results are given in table 9. These results show differences from expected compositions ranging from 5 to 25 relative percent. The problem is compounded by the fact that deviations of the probe analyses from expected compositions are positive in two cases and negative in the other two. Hence, the expected compositions are not consistent among themselves. The manganiferous glass was considered adequate for estimating the manganese contents of kimberlite diopsides which usually contain $\sim$0.1 percent MnO, but clearly the uncertainty in the Mn analyses is at least $\pm$5-10 relative percent.

The diopside inclusions from kimberlite also contain small amounts of Ti and K. An orthoclase analyzed and provided by C. O. Ingamells was used as a potassium standard. For Ti, a glass on the join $CaMgSi_2O_6$–TiO_2 containing 2.00 percent TiO_2 was prepared by the author, using J. F. Schairer's techniques.

TABLE 8

Analyses for Na in natural jadeite and in two glasses on the join diopside-jadeite, with a third glass* on this join as a standard

	Matrix correction	Weight percent Na	
		Probe	Expected
$Di_{95}Jd_5$	1.023	0.57	0.57
$Di_{85}Jd_{15}$	1.021	1.73	1.71
Jadeite†	0.945	11.0	10.66

*Composition $Di_{65}Jd_{35}$.

†USNM 94829; analysis by E. G. Zies (Yoder, 1950).

TABLE 9

Analyses for Mn in various natural minerals, with a glass on the join $Mg_3Al_2Si_3O_{12}$-$MnSiO_3$ as a standard*

	$\sigma/\sqrt{\bar{N}}$	Matrix correction	Weight percent Mn	
			Probe	Expected
Spessartite	1	0.950	31.4	33.38
Cummingtonite	25	0.977	0.84	0.75
Magnetite	3	1.119	0.38	0.30
Diopside	...	1.015	0.09	0.10

*The glass contains 4.19 weight percent Mn.
σ = standard deviation.
$\bar{N}$ = mean count.
Spessartite, Wodgina (Mason and Berggren, 1941).
Cummingtonite, Mikonui (Mason, 1953).
Magnetite, L4-175.
Diopside, Thaba Putsoa, E-3 (Nixon, von Knorring, and Rooke, 1963).

Analytical Techniques

Samples studied in this investigation included diopside-bearing nodules, single pyroxene crystals, and one grain aggregate partially purified for wet-chemical analysis. Most of the nodules were prepared for probe study as polished thin sections. The majority of the single crystals were hand-picked from pulsator concentrates and mounted in standard metallurgical mounts. All mounts were carbon-coated with a coat thickness corresponding to a purple-blue color on polished brass (Smith, 1965).

Where whole nodules were available, attempts were made to obtain representative compositions for the contained diopside. In such cases, counts were made on three to twelve grains, although differences between grains in a given nodule are usually small. In general, considerably more data were obtained on the samples for which complete analyses are reported than on the larger number of specimens of which only partial analyses were made.

TABLE 10

Operating conditions for analyses in table 2

	Kv	$\underline{i}$*	Counts/sec	Line/background†	Counting time, sec.	Points analyzed	Analyzing crystal
Si	15	0.02-0.05	2000-5000	200-300	10-20	40-170	KAP
Ti	15	0.1	60-100	1.01-3.0	100	15-20	PET
Al	15	0.1-0.2	350-600	20-30	100	15-30	KAP
Cr	20	0.1	600-2000	6-14	30-50	20-40	PET
Fe	20	0.1	350-700	11-25	30-50	23-40	LiF
Mn	20	0.2	50-70	1.5-2	100	20-25	LiF
Ca	15	0.03-0.06	850-2000	200-300	20-30	40-80	PET
Mg	15	0.03-0.06	500-1000	200-300	20-30	40-80	KAP
Na	15	0.1	50-120	5-25	100	17-40	KAP
K	15	0.1-0.2	12-33	1.01-2.0	100	15-30	PET

*$\underline{i}$ = sample current, μa.

†Si analyses were made with no slit on detector. All others were made with 20-mil slit and pulse-height analyzer windows set to pass >95 percent of signal.

Operating conditions for the complete analyses are summarized in table 10. Similar conditions were used for the partial analyses except that the number of points analyzed was only five to ten. In most cases the beam size was set at approximately 10 μm. These are coarse-grained minerals, and there was usually no advantage in using a smaller beam. The diopside inclusion from diamond (sample M) had rather restricted areas where the polish was good, however, and analyses were made with a beam size in the range 1 to 2 μm.

Corrections for background are small for analyses of major elements, and in such cases, backgrounds were counted at two positions, 0.050 to 0.100 Å upscale and down-scale from the peak positions, and averaged. However, careful measurement of background is essential for the analysis of elements present in low concentrations. Counting background on blanks with mean atomic numbers similar to the unknowns was attempted but abandoned. This procedure can lead to serious errors unless account is taken of pronounced differences in the absorption of background radiation by different elements in a multi-element target (V. G. Macres, unpub. ms). Background measurements for a given wavelength can be very different on two targets that differ in composition but have identical mean atomic numbers. Accordingly, background intensities for Mn, Fe, Cr, Ti, K, and Al were determined by scanning on the samples for which complete analyses were made. Counts were taken at ten points ranging from 0.050 Å above to 0.050 Å below each peak position on each specimen. These data were plotted, and graphical extrapolations gave ratios between background at peak position and background at an arbitrary point up-scale from the peak. Background counts were taken at these selected points during analysis, and the intensities were then adjusted by the predetermined ratios. Less careful determinations of background for Fe, Cr, and Al were made on the samples that were only partially analyzed. Usually, a number of these specimens were analyzed

in sequence, and background counts were obtained above and below peak for a few representative samples in each sequence.

The drift correction was made by averaging counts on the standards taken before and after counts on an unknown. Analyses were discarded if the drift was greater than 3 percent. Drift was found to be nonlinear with time, and commonly it varied in magnituude and sign among the three read-out channels. Hence, more elaborate drift corrections which apportion drift as a function of time seemed unrealistic.

References

Boyd, F. R., 1967, Electron probe study of diopside pyroxenes from kimberlites: Carnegie Inst. Washington Year Book 65, p. 252-260.

———— 1968, Quantitative electron-probe analysis of pyroxenes: Carnegie Inst. Washington Year Book 66, p. 327-334.

Boyd, F. R., and England, J. L., 1964, The system enstatite-pyrope: Carnegie Inst. Washington Year Book 63, p. 157-163.

Boyd, F. R., Finger, L. W., and Chayes, Felix, 1968, Computer reduction of electron-probe data: Carnegie Inst. Washington Year Book 67, in press.

Davis, B. T. C., and Boyd, F. R., 1966, The join $Mg_2Si_2O_6$–$CaMgSi_2O_6$ at 30 kilobars pressure and its application to pyroxenes from kimberlites: Jour. Geophys. Research, v. 71, p. 3567-3576.

Duncumb, P., and Reed, S. J. B., 1968, Progress in the calculation of stopping power and backscatter effects, *in* Heinrich, Kurt, ed., Quantitative electron-probe microanalysis: Natl. Bur. Standards Spec. Tech. Pub., in press.

Duncumb, P., and Shields, P. K., 1963, The present state of quantitative X-ray microanalysis, Part 1, Physical basis: British Jour. Appl. Physics, v. 14, p. 617-627.

Heinrich, K. F. J., 1966, X-ray absorption uncertainty, *in* McKinley, T. D., Heinrich, K. F. J., and Wittry, D. B., ed., The electron mircoprobe: New York, John Wiley & Sons, Inc., p. 296-377.

Holmes, A., 1936, Contributions to the petrology of kimberlite and its inclusions: Geol. Soc. South Africa Trans. Proc., v. 39, p. 379-428.

Kushiro, I., 1968, Synthesis and stability of iron-free pigeonite in the system $MgSiO_3$–$CaMgSi_2O_6$ at high pressures: Carnegie Inst. Washington Year Book 67, in press.

Kushiro, I., Syono, Y., and Akimoto, S., 1967, Effect of pressure on garnet-pyroxene equilibrium in the system $MgSiO_3$–$CaSiO_3$–Al_2O_3: Earth and Planetary Sci. Letters, v. 2, p. 400-464.

MacGregor, I. D., 1964, The reaction 4 enstatite + spinel ⇄ forsterite + pyrope: Carnegie Inst. Washington Year Book 63, p. 157.

———— 1965, Stability fields of spinel and garnet peridotites in the synthetic system MgO–CaO–Al_2O_3–SiO_2: Carnegie Inst. Washington Year Book 64, p. 126-134.

MacGregor, I. D., and Ringwood, A. E., 1964, The natural system enstatite-pyrope: Carnegie Inst. Washington Year Book 63, p. 161-163.

Mason, B. H., 1953, Cummingtonite from the Mikonui River, Westland, New Zealand: Am. Mineralogist, v. 38, p. 862-865.

Mason, B. H., and Berggren, T., 1941, A phosphate-bearing spessartite garnet from Wodgina, western Australia: Geol. Fören. Stockholm Förh., v. 63, p. 413-418.

Meyer, H. O. A., 1968, Chrome pyrope: An inclusion in natural diamond: Science, v. 160, p. 1446-1447.

Nixon, P. H., von Knorring, O., and Rooke, J. M., 1963, Kimberlites and associated inclusions of Basutoland, a mineralogical and geochemical study: Am. Mineralogist, v. 48, p. 1090-1132.

O'Hara, M. J., and Mercy, E. L. P., 1963, Petrology and petrogenesis of some garnetiferous peridotites: Roy. Soc. Edinburgh Trans., v. 65, p. 251-314.

O'Hara, M. J., and Yoder, H. S., Jr., 1967, Formation and fractionation of basic magmas at high pressures: Scottish Jour. Geology, v. 3, p. 67-117.

Philibert, J. A., 1963, A method for calculating the absorption correction in electron-probe microanalysis, *in* Pattee, H. H., Jr., Cosslett, V. E., and Engström, A., ed., Third International symposium on X-ray optics and microanalysis: New York, Academic Press, p. 379-392.

Reed, S. J. B., 1965, Characteristic fluorescence corrections in electron-probe microanalysis: British Jour. Appl. Physics, v. 16, p. 913-926.

Smith, J. V., 1965, X-ray emission microanalysis of rock-forming minerals, 1. Experimental techniques: Jour. Geology, v. 73, p. 830-864.

Yoder, H. S., Jr., 1950, The jadeite problem: Am. Jour. Sci., v. 248, p. 225-248, 312-334.